Pyroliton: pyroelectric spatial soliton

Jassem Safioui, Fabrice Devaux, and Mathieu Chauvet*

Département d'Optique, Institut FEMTO-ST, UMR CNRS 6174, Université de Franche-Comté, 25030 Besançon, France

**mathieu.chauvet@univ-fcomte.fr*

Abstract: The concept of optical beam self-trapping in pyroelectric photorefractive medium is presented. We show that the temperature controlled spontaneous polarisation of ferroelectric crystals produces an optical nonlinearity that can lead to formation of 2-D spatial soliton named pyroliton. Experimental demonstrations performed in lithium niobate crystals illustrate that efficient self-trapping occurs either for ordinary or extraordinary polarisation under moderate temperature increase. For instance, a 15µm diameter pyroliton can be formed with a 10 degree temperature raise.

OCIS codes: (190.5330) Photorefractive optics; (190.6135) Spatial solitons.

References and links

1. R. Y. Chiao, E. Garmire, and C. H. Townes, "Self-Trapping of Optical Beams," Phys. Rev. Lett. **13**(15), 479–482 (1964).
2. A. Barthélémy, S. Maneuf, and C. Froehly, "Propagation soliton et auto-confinement de faisceaux laser par non linearité optique de Kerr," Opt. Commun. **55**(3), 201–206 (1985).
3. K. Hayata, and M. Koshiba, "Multidimensional solitons in quadratic nonlinear media," Phys. Rev. Lett. **71**(20), 3275–3278 (1993).
4. M. Peccianti, A. De Rossi, G. Assanto, A. De Luca, C. Umeton, and I. C. Khoo, "Electrically assisted self-confinement and waveguiding in planar nematic liquid crystal cells," Appl. Phys. Lett. **77**(1), 7–9 (2000).
5. G. C. Duree, Jr., J. L. Shultz, G. J. Salamo, M. Segev, A. Yariv, B. Crosignani, E. J. Sharp, R. R. Neurgaonkar, and P. Di Porto, "Observation of self-trapping of an optical beam due to the photorefractive effect," Phys. Rev. Lett. **71**(4), 533–536 (1993).
6. A. D. Boardman, and A. P. Sukhorukov, *Soliton Driven Photonics* (Kluwer Acad. Publ., Dordrecht, 2001).
7. S. Trillo, and W. E. Torruellas, *Spatial Solitons* (Springer-Verlag, Berlin, 2001).
8. M. Segev, G. C. Valley, B. Crosignani, P. Di porto, and A. Yariv, "Steady-State Spatial Screening Solitons in Photorefractive Materials with External Applied Field," Phys. Rev. Lett. **73**(24), 3211–3214 (1994).
9. M. Morin, G. C. Duree, G. J. Salamo, and M. Segev, "Waveguides formed by quasi-steady-state photorefractive spatial solitons," Opt. Lett. **20**(20), 2066–2068 (1995).
10. D. Neshev, E. Ostrovskaya, Y. Kivshar, and W. Krolikowski, "Spatial solitons in optically induced gratings," Opt. Lett. **28**(9), 710–712 (2003).
11. W. Królikowski, M. Saffman, B. Luther-Davies, and C. Denz, "Anomalous Interaction of Spatial Solitons in Photorefractive Media," Phys. Rev. Lett. **80**(15), 3240–3243 (1998).
12. E. Fazio, F. Renzi, R. Rinaldi, M. Bertolotti, M. Chauvet, W. Ramadan, A. Petris, and V. I. Vlad, "Screening-photovoltaic bright solitons in lithium niobate and associated single mode waveguides," Appl. Phys. Lett. **85**(12), 2193–2195 (2004).
13. M. Taya, M. C. Bashaw, M. M. Fejer, M. Segev, and G. C. Valley, "Observation of dark photovoltaic spatial solitons," Phys. Rev. A **52**(4), 3095–3100 (1995).
14. W. L. She, K. K. Lee, and W. K. Lee, "Observation of Two-Dimensional Bright Photovoltaic Spatial Solitons," Phys. Rev. Lett. **83**(16), 3182–3185 (1999).
15. C. Anastassiou, M. F. Shih, M. Mitchell, Z. Chen, and M. Segev, "Optically induced photovoltaic self-defocusing-to-self-focusing transition," Opt. Lett. **23**(12), 924–926 (1998).
16. J. D. Brownridge, "Pyroelectric x-ray generator," Nature **358**(6384), 277–278 (1992).
17. J. Geuther, Y. Danon, and F. Saglime, "Nuclear Reactions Induced by a Pyroelectric Accelerator," Phys. Rev. Lett. **96**(5), 054803–054806 (2006).
18. S. M. Kostritskii, O. G. Sevostyanov, M. Aillerie, and P. Bourson, "Suppression of photorefractive damage with aid of steady-state temperature gradient in nominally pure LiNbO3 crystals," J. Appl. Phys. **104**(11), 114104–114114 (2008).
19. P. Günter, and J. P. Huignard, *Photorefractive materials and their applications 2* (Springer, Berlin, 2007).
20. F. Devaux, V. Coda, M. Chauvet, and R. Passier, "New time-dependent photorefractive three-dimensional model: application to self-trapped beam with large bending," J. Opt. Soc. Am. B **25**(6), 1081–1086 (2008).

#117378 - $15.00 USD Received 17 Sep 2009; revised 15 Oct 2009; accepted 26 Oct 2009; published 19 Nov 2009

21. T. Bartholomaüs, K. Buse, C. Deuper, and E. Krätzig, "Pyroelectric Coefficients of LiNbO3 Crystals of Different Compositions," Phys. Status Solidi **142**(1), K55–K57 (1994) (a).
22. A. Savage, "Visual system-response functions and estimating reflectance," J. Appl. Phys. **37**, 3071 (1966).
23. M. Simon, S. Wevering, K. Buse, and E. Krätzig, "The bulk photovoltaic effect of photorefractive $LiNbO_3$:Fe crystals at high light intensities," J. Phys. D **30**(1), 144–149 (1997).
24. J. Safioui, M. Chauvet, F. Devaux, V. Coda, F. Pettazzi, M. Alonzo, and E. Fazio, "Polarization and configuration dependence of beam self-focusing in photorefractive liNbO3," J. Opt. Soc. Am. B **26**(3), 487–492 (2009).
25. A. A. Zozulya, and D. Z. Anderson, "Propagation of an optical beam in a photorefractive medium in the presence of a photogalvanic nonlinearity or an externally applied electric field," Phys. Rev. A **51**(2), 1520–1531 (1995).
26. G. Montemezzani, C. Medrano, and P. Günter, "Charge carrier photoexcitation and two-wave mixing in dichroic materials," Phys. Rev. Lett. **79**(18), 3403–3406 (1997).

1. Introduction

Since the prediction of beam self-trapping more than 40 years ago [1] followed by the first observation of stable trapping by Kerr effect 20 years later [2], the quest for more versatile and efficient nonlinear focusing medium remains. Quadratic medium [3], liquid crystals [4] or photorefractive (PR) medium [5] are able to give rise to self-confined beams that keep a constant transverse profile upon propagation. Such beams called spatial solitons [6, 7] have also been named specifically depending on the configuration. For instance *Simultons* applies to two frequency components solitons and *Nematicons* are formed in nematic liquid crystals. Photorefractive spatial solitons have attracted much attention [8–11] because of their appealing features. For instance, they can be created at very low light power level and are stable in 2-D due to the saturating character of the nonlinearity. Nevertheless, application of a strong external applied electric field is, most often, a necessary condition to obtain the local PR nonlinearity required in light trapping experiments [12]. This drawback is not present in the case of photovoltaic photorefractive crystals [13, 14] but control of the photorefractive nonlinearity sign and amplitude is challenging [15] since the photovoltaic field is intrinsic to the crystal and is primarily intensity independent. In this paper we instead propose to use the spontaneous polarisation of ferroelectric crystal to induce a nonlinear optical effect which can be controlled using the pyroelectric effect. The concept of pyroelectric photorefractive solitons that can be formed by simple adjustment of the PR crystal temperature is introduced. Experimental demonstrations performed in lithium niobate ($LiNbO_3$) samples are presented.

2. Theoretical model

Pyroelectric crystals exhibit a variation in spontaneous polarisation P_s as a function of temperature change given by its pyroelectric coefficient $p=\partial Ps/\partial T$. In short-circuit crystal this spontaneous polarisation change is known to induce transient electric currents fruitfully utilized in wide bandwidth pyroelectric photodetectors. In open-circuit configuration very high electric field can be generated by pyroelectric effect. Such large electric field induced in the surrounding of pyroelectric crystal can be used to ionise and accelerate charged particles [16-17]. Recently, steady-state temperature gradient was shown to suppress photorefractive damage in $LiNbO_3$ [18]. In this letter internal electric field generated by a temperature change DT in an open-circuit crystal is considered. This electric field variation E_{py} due to the spontaneous polarisation change is given by:

$$E_{py} = \Delta E = -\frac{1}{\varepsilon_0 \varepsilon_r} p \, \Delta T. \qquad (1)$$

where ε_0 and ε_r are the vacuum and relative dielectric constants, respectively. Note that in a ferroelectric crystal at equilibrium the net internal field inside the crystal is null since the field due to spontaneous polarisation is compensated by charges accumulated on crystal faces. However temperature change induces direct spontaneous polarisation variation and thus electric field E_{py}. This field is not immediately compensated and a drift current can consequently take place as if an external voltage was applied to the crystal. The idea behind

#117378 - $15.00 USD Received 17 Sep 2009; revised 15 Oct 2009; accepted 26 Oct 2009; published 19 Nov 2009

the concept of pyroelectric spatial soliton is to locally screen this initial homogeneous pyroelectric electric field E_{py} using the PR effect in order to induce beam self-trapping. Several conditions have to be fulfilled to allow beam self-focusing. For instance, once a crystal temperature is set, the induced pyroelectric field has to remain long enough compare to PR response time. Charge sorption on the polar surface of the crystal that progressively tends to compensate the temperature induced E_{py} has thus to be slower than the response time of the light-induced beam self-trapping. Moreover, the amplitude of E_{py} has to be large enough to induce efficient trapping for a moderate temperature change compatible with PR effect.

To model beam self-trapping in pyroelectric photorefractive crystal we consider a time-dependent band-transport model [19] with a single deep trap. Electrons which are dominant free charges are displaced by photovoltaic effect and under drift current along the crystal c-axis while diffusion is neglected. An open-circuit crystal at homogeneous and steady temperature is considered.

When illuminated with a light intensity distribution I, evolution of the charge density r is given by:

$$\frac{\partial \rho}{\partial t} = -\mu e \vec{\nabla}\left(N.\vec{E}\right) - \beta_{ph}\vec{\nabla}[(N_d - N_d^+)I]\cdot\vec{c}. \tag{2}$$

where free electron density N, ionized donor density N_d^+ and internal electric field $\vec{E}$ are given by Eqs. (3), (4) and (5), respectively

$$N = \frac{s(I+I_d)(N_d - N_d^+)}{\gamma N_d^+}. \tag{3}$$

$$N_d^+ = N_a + \frac{\rho}{e}. \tag{4}$$

$$\vec{E}(\vec{r}) = E_{py}.\vec{c} + \frac{1}{4\pi\varepsilon_0\varepsilon_r}\iiint_V \rho(\vec{r}')\frac{\vec{r}-\vec{r}'}{\left|\vec{r}-\vec{r}'\right|^3}dV. \tag{5}$$

N_d is the total donor density; N_a is the density of ionized shallow acceptors. $I_d=\beta/s$ is the equivalent dark irradiance with β and s the thermal and photoexcitation coefficients, γ is the recombination coefficient, μ is the electron mobility, β_{ph} is the photovoltaic coefficient and e is electron charge. Note that temperature change of the crystal due to illumination is neglected.

The electric field evolution is obtained by solving iteratively the set of Eq. (2-5) [20] in conjunction with the wave propagation equation. Starting from initial conditions, the electron density is calculated from Eq. (3) and space charge variation after a time step Δt is deduced from Eq. (2). Then the ionized donor density is obtained from Eqs. (4). The electric field is deduced from Eq. (5). The inferred 2-D refractive index perturbation Δn due to linear electro-optic effect is finally used to calculate light propagation along y-axis in the perturbed medium by a classical split-step Fourier transform method according to the nonlinear propagation equation.

$$\left\{\frac{\partial}{\partial y} - \frac{i}{2k}\Delta_\perp\right\}A = i\,k\Delta n\,A. \tag{6}$$

where $\Delta_\perp = \partial^2/\partial x^2 + \partial^2/\partial z^2$ is the transverse operator, A is the slowly-varying amplitude of the light field and k is the wavenumber in the medium.

#117378 - $15.00 USD Received 17 Sep 2009; revised 15 Oct 2009; accepted 26 Oct 2009; published 19 Nov 2009

To illustrate the concept of pyroelectric beam self-trapping we selected the widely available ferroelectric $LiNbO_3$ crystal. It possesses well-known PR properties along with a pyroelectric coefficient p close to -6.10^{-5} C m^{-2} K^{-1} at 25°C [21, 22]. The pyroelectric field E_{py} is oriented along the crystal c-axis (z-axis) and can be either positive or negative by increase or decrease of the crystal temperature, respectively. From Eq. (1) an amplitude of 47 kV/cm can be deduced for the internal pyroelectric electric field E_{py} under a temperature increase of 20°C. A linearly polarized beam propagating along the crystal y-axis can sense the light-induced refractive index distribution $\Delta n=-0.5n^3 r_{eff}E_z$. Where E_z is the electric field component along the crystal c-axis, n is average refractive index and r_{eff} is the effective electro-optic coefficient. Two configurations are analyzed, n_o=2.3 and r_{13}=8pm/V for ordinary polarized light and n_e=2.2 and r_{33}=31pm/V for extraordinary polarized light. Undoped $LiNbO_3$ crystals are used for the experimental demonstration and a single iron deep center is considered in the model. Corresponding parameters are taken from ref [23].

Figure 1 depicts the predicted behavior of an extraordinary polarized beam, with a 16µm (FWHM) width at the entrance face, propagating in a 20 mm long $LiNbO_3$ crystal whose temperature has been raised 10°C above initial temperature. When light is switched on progressive self-focusing is observed (Fig. 1(c)) until best confinement is reached (Fig. 1(d)).

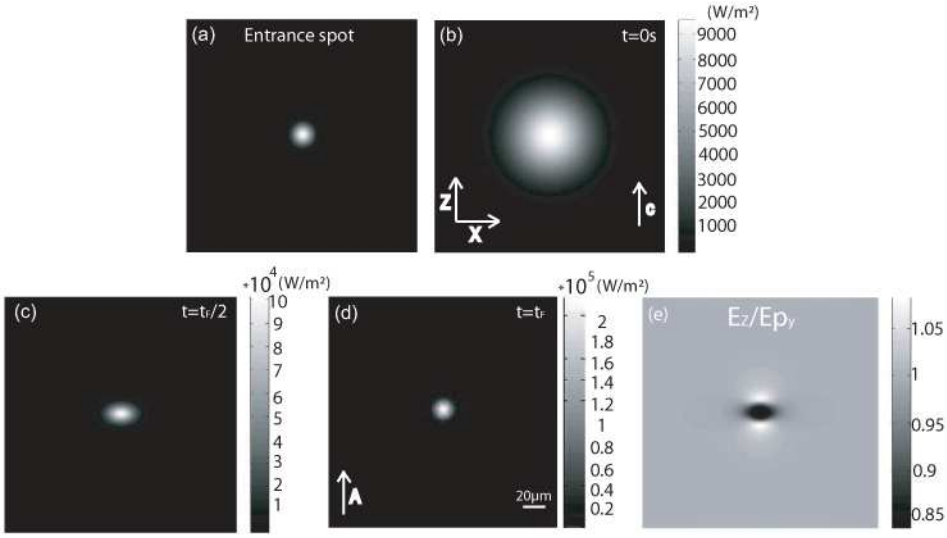

Fig. 1. Numerical calculation of pyroelectric beam self-trapping for an extraordinary polarised beam in a 20 mm long crystal. Intensity distribution at the input face (a), output face in linear regime (b), output face in nonlinear regime at $t=t_F$ for best focusing (d) and at $t=t_F/2$ (c). Corresponding z-component of the electric field distribution normalized to E_{py} at exit face at $t=t_F$. Parameters: 80µw beam power, 16µm input beam FWHM, DT=10°C, E_{ph}=19kV/cm.

The z-component distribution of the electric field, at the heart of the self-confinement process, is depicted in Fig. 1(e). Away from the beam location the electric field is equal to E_{py} while in the central part of the beam lower amplitude is obtained because of the presence of the photorefractive space charge field. Note that the minimum field amplitude approaches the photovoltaic field amplitude $E_{ph}=\beta\gamma N_A/(e\mu s)$. Therefore E_{ph} depends on light polarization [24] through photovoltaic coefficient β_{ph} and on crystal doping concentration. In the presented simulation E_{ph} is set to 19kV/cm for extraordinary polarization. Since the index change is proportional to the opposite of the electric field it thus results that a waveguide structure is created in the crystal providing E_{py} is larger than E_{ph}. Moreover anisotropy of the effect is characterized by the two local minima present along the c-axis which are typical of a two-dimensional charge distribution as earlier observed for screening solitons [25]. This anisotropic index distribution usually gives a slightly elliptical beam with a stronger confinement along c-axis. Note that for chosen parameters a circular beam with a similar size

#117378 - $15.00 USD Received 17 Sep 2009; revised 15 Oct 2009; accepted 26 Oct 2009; published 19 Nov 2009

than the launched beam (16µm FWHM) is present at the exit face of the crystal when best confinement (Fig. 1(a), 1(d)) is reached which corresponds to a solitonic propagation. For parameters corresponding to an ordinary polarized beam (not shown) confinement is also observed. However the weaker adverse photovoltaic field and the electrooptic coefficient which is about 4 times lower than for extraordinary light give only partial beam diffraction compensation.

3. Experiments

For the experimental demonstration either undoped photonic grade congruent or stoichiometric $LiNbO_3$ crystals are used. Samples cut from photonic grade z-cut wafers have dimensions 8×20×0.5 mm^3 along x, y and z crystallographic axes, respectively. The sample under test is placed between an insulating plastic cover and a metallic plate whose temperature is accurately controlled by a Peltier element. Such an arrangement provides a homogeneous temperature of the crystal with stability better than 0.1°C. Input and output faces of the crystal are observed on a CCD camera via imaging lenses.

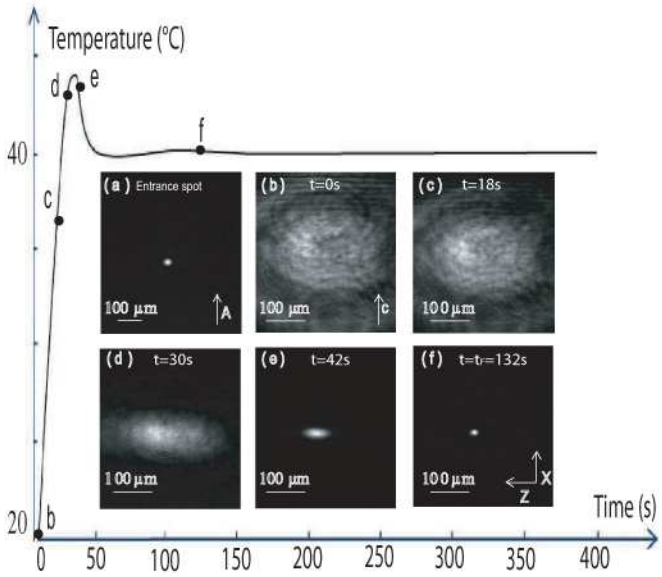

Fig. 2. Pyroelectric self-focusing dynamics of an extraordinary polarized beam at λ=532 nm in a 20mm long stoichiometric $LiNbO_3$ crystal. Crystal temperature evolution (curve) and images at the input face (a) and at the output face at different instant indicated on the curve (b-f). Parameters: 80µW input beam power, 11 µm input beam FWHM.

A first experiment is performed with an extraordinary polarised light in a stoichiometric $LiNbO_3$ crystal. A 532nm CW beam is focused to an 11µm FWHM spot at the front face and propagates over 20mm along the $LiNbO_3$ y-axis direction. When the crystal is at room temperature the beam diffracts along propagation, its width at the output face approaches the crystal 500 µm thickness (Fig. 2(b)) as witnessed by the Lloyd interferences produced by reflection on each side of the crystal. Moreover its spatial distribution is not Gaussian since no spatial filter was used to clean the launched beam. Nevertheless when the crystal temperature start to rise from room temperature to 40°C the 80µW beam self-focuses progressively. As shown in Fig. 2(d) beam confinement and clean-up are already obvious after 1 min of exposure while crystal temperature is not yet stabilized. As predicted by the numerical model, trapping is more efficient along the z-axis than along x-axis which is clearly observed in Fig. 2(e). When maximum confinement ($t=t_F$) is reached a smooth and efficiently focused spot is obtained (Fig. 2(f)) with a 7 µm FWHM along c-axis and a 8 µm FWHM along x-axis. The large initial beam diffraction has thus been overcompensated which

#117378 - $15.00 USD Received 17 Sep 2009; revised 15 Oct 2009; accepted 26 Oct 2009; published 19 Nov 2009

illustrates the remarkable self-trapping efficiency triggered by the spontaneous polarisation of the crystal. Note that self-trapping can also be obtained when crystal temperature is stabilized for several minutes before beam is switched turned on. Since this procedure is more consistent with the assumptions of our theoretical model it is used as a standard procedure in the following experiments. Assessment of the focusing strength at different time after temperature is set leads to an internal pyroelectric field decay rate τ of about 8h in our lithium niobate crystals. This slow decay due to the compensation of E_{py} is consistent with the dielectric response time of $LiNbO_3$ in the dark.

To illustrate the influence of temperature change on self-trapping strength, the output beam width as a function of temperature variation ΔT has been measured. Results are depicted in Fig. 3. Starting from room temperature, the crystal temperature is gradually raised. The beam FWHM is measured both perpendicular and along c-axis for best focusing at $t=t_F$. Focusing strength increases with temperature to initially form an elliptical spot that gradually transforms to a round spot at $\Delta T=12°C$. Larger temperature change tends to distort the trapped beam.

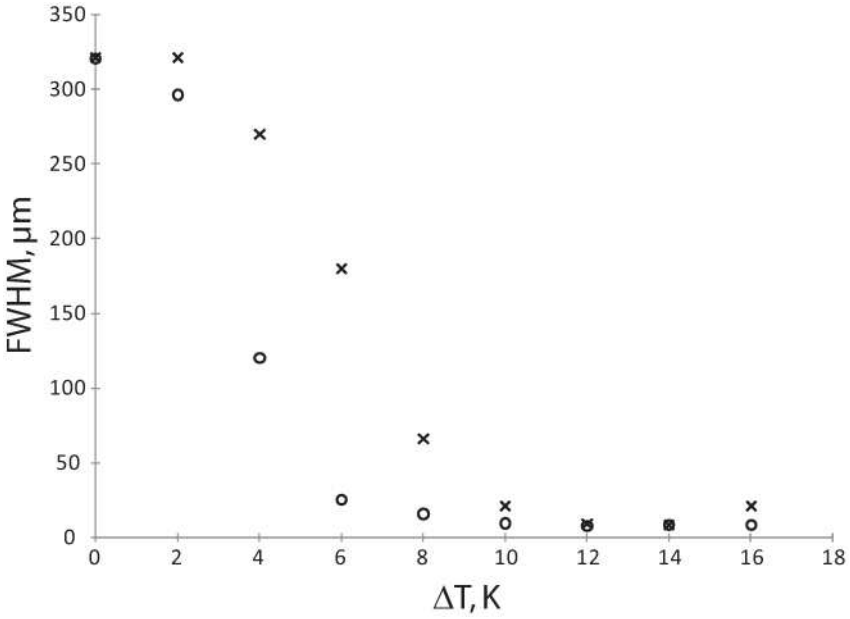

Fig. 3. Beam FWHM perpendicular (crosses) and along c-axis (circles) at the output face of a 20mm long congruent $LiNbO_3$ crystal as a function of temperature increase. Parameters: 30µW input beam power, 12 µm input beam FWHM, 273K initial temperature, extraordinary polarisation, λ=532 nm

Additional results obtained in congruent $LiNbO_3$ samples show similar behaviour than in stoichiometric samples. As an illustration and, in the meantime, to show the influence of light polarisation, two sets of experiment performed in congruent $LiNbO_3$ are presented in Fig. 4. It comes into view that optimum confinement leads to tighter beam for extraordinary polarisation (Fig. 4(d)) than for ordinary polarisation (Fig. 4(c)) as expected from theory. Uncertainties on the value of crystal parameters prohibit quantitative prediction of the time evolution but the overall behaviour is correctly described by our numerical calculation. Note that the induction time to reach best focusing ($t=t_F$) is dependent on light polarization. t_F=3 min (Fig. 4(d)) or t_F=9 min (Fig. 4(c)) for extraordinary or ordinary polarisation, respectively. This response time disparity can be attributed to the photorefractive field which has larger amplitude for ordinary light and thus takes a longer time to build-up [24]. In addition the photoionization cross section can be polarisation dependent because of crystal anisotropy [26].

#117378 - $15.00 USD Received 17 Sep 2009; revised 15 Oct 2009; accepted 26 Oct 2009; published 19 Nov 2009

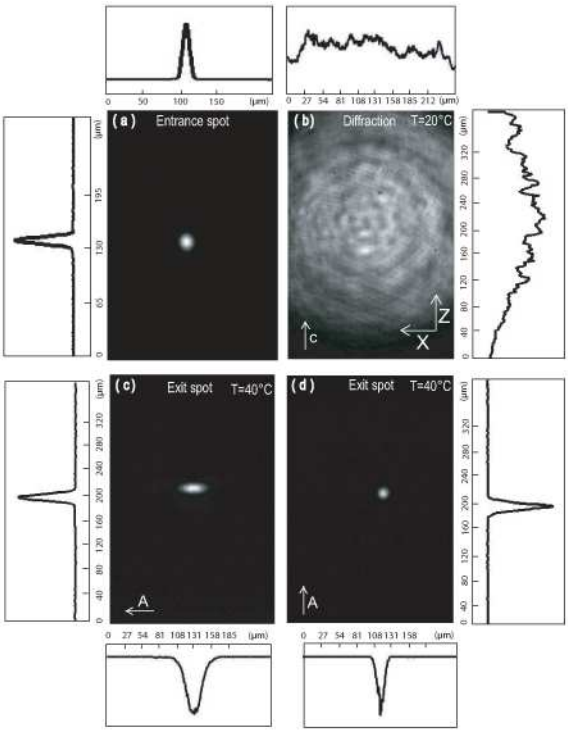

Fig. 4. Pyroelectric self-trapping in a 20 mm long congruent $LiNbO_3$ sample for ordinary and extraordinary polarised beams. Image at the entrance face (a), at the exit face in diffraction regime (b) and in nonlinear regime with ordinary (t_F=9min) (c) or extraordinary (t_F=3min) (d) polarisations. Parameters: 80µW input beam power, 15µm input beam FWHM, ΔT=20°C.

For a given temperature change DT, which is the experimental parameter that dictates the amplitude of the nonlinear effect, the beam profile to launch in order to obtain propagation with an invariant transverse profile can be determined. Such a solitonic propagation is depicted in the numerical results in Fig. 1. The corresponding experimental demonstration of a spatial soliton supported by crystal spontaneous polarisation is shown in Fig. 5. An extraordinary polarized 15µm FWHM pyroliton is obtained when crystal temperature is raised 10°C above room temperature as witnessed by the similar beam profile at the input (Fig. 5(a)) and output (Fig. 5(b)) face of the crystal. Note that these solitons are obtained in quasi-steady-state regime [9] since longer exposure time shows beam broadening. A solution to form steady-state narrow solitons could be to artificially increase the dark irradiance with the help of a uniform background illumination as for screening solitons [8]. Also note that once spatial soliton is formed, beam can be switched off and crystal can be reset to room temperature without altering the induced guiding structure. Due to the high resistivity of $LiNbO_3$ long living waveguides are thus memorised in the crystal and can thus be practically used to guide low power beams at different wavelengths. Indeed photorefractive effect is negligible for low power visible beam or at near I. R. telecommunication wavelengths. In such a situation induced waveguides are memorized even if $LiNbO_3$ sample temperature changes.

#117378 - $15.00 USD Received 17 Sep 2009; revised 15 Oct 2009; accepted 26 Oct 2009; published 19 Nov 2009

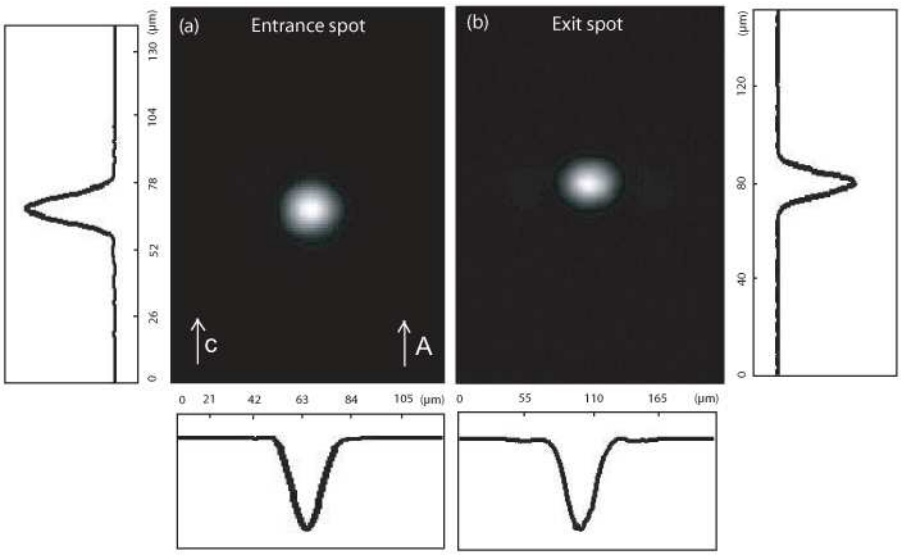

Fig. 5. Experimental demonstration of a pyroliton in $LiNbO_3$. Input (a) and output (b) beam intensity distribution. Parameters: 80μW input beam power, 15μm beam FWHM, ΔT=10°C.

4. Conclusion

The concept of beam self-trapping using spontaneous polarisation of ferroelectric crystal has been presented. Amplitude and sign of the nonlinear focusing effect is simply triggered and controlled by crystal temperature via the pyrolectric effect. Experimental demonstrations have been performed in $LiNbO_3$ crystals and spatial solitons, named pyroliton, have been obtained. Photonic grade undoped congruent or stoichiometric $LiNbO_3$ samples reveal efficient beam self-confinement under moderate temperature change on the order of 10°C. This powerful and easy to control optical nonlinearity can be advantageously employed to induce structures such as gratings, complex lattices or 3-D integrated circuits even inside large size medium. It is important to note that the reported effect could potentially be obtained in other pyroelectric photorefractive crystals providing characteristics such as long pyroelectric field decay time and large enough pyroelectric field amplitude are present.

#117378 - $15.00 USD Received 17 Sep 2009; revised 15 Oct 2009; accepted 26 Oct 2009; published 19 Nov 2009